STUDY TO OBTAIN UHPC WITH ADDITION OF SILICA AND MGW

Priscila de Souza Maciel[1,2], Maria Luiza Malta da Rocha Silva[1], Ingrid Vieira Fernandes Monteiro[1] and Paulo Cesar Correia Gomes[1]
[1]Universidade Federal de Alagoas, Maceió/AL, Brasil
[2] Instituto Federal de Educação, Ciência e Tecnologia de Alagoas, Maceió/AL, Brasil
priscila.maciel@ifal.edu.br
[1]Universidade Federal de Alagoas, Maceió/AL, Brasil
maria.rocha@ctec.ufal.br
[1]Universidade Federal de Alagoas, Maceió/AL, Brasil
ingrid_vfmonteiro@hotmail.com
[1]Universidade Federal de Alagoas, Maceió/AL, Brasil
pgomes@ctec.ufal.br

ABSTRACT

Ultra-high performance concrete (UHPC) is a specialized concrete with high durability and compressive strength due to its dense structure and low porosity. This study investigated UHPC mixtures with mineral and chemical additions to meet the regulatory parameters for classification as UHPC at 56 days: spread of 270 mm, flexural tensile strength of 6 MPa, and compressive strength of 120 MPa. Variations in Marble and Granite Waste (MGW), silica, superplasticizer, and water were studied. MGW and sand characterization was performed. Consistency and volumetric/mass variation were analyzed in the fresh state, while flexural tensile and compressive strengths were examined in the hardened state. The best-performing mix, with 50% MGW, 20% silica, 1.5% superplasticizer, and w/b=0.25, had the best performance, exhibiting minimum values at 56 days, reaching 130 MPa compressive strength at 91 days, highlighting the potential of MGW and silica in UHPCs.

KEYWORDS: *Ultra-High Performance Concrete, Silica & MGW.*

I. INTRODUCTION

To achieve high-performance structures that use inputs efficiently and meet regulatory standards, even in the most extreme environments, ultra-high performance concretes (UHPCs) show great potential in civil construction due to their excellent mechanical properties and durability [1]. UHPC combines the properties of high-performance concrete and self-compacting concrete, offering high mechanical strength and workability, among other advantages [2].

Ultra-high performance materials are typically composed of cement, quartz powder, fly ash, silica fume, quartz sand, superplasticizers, and steel fibers [3]. The high compactness and density of the UHPC matrix contribute to its excellent performance, as well as its low permeability, which reduces susceptibility to aggressive agents and enhances durability.

UHPCs possess compressive strength greater than 120 MPa and tensile strength exceeding 6 MPa after 56 days of curing, while maintaining good workability, with a spread range of 270 mm[4]. Achieving these properties requires a low water/binder ratio (w/b), a high superplasticizer content, the use of high-speed mixers, and a dense cementitious matrix [5] .

The packing factor is crucial in distinguishing UHPC from conventional concrete [6]. Packing involves optimizing grain size distribution within the mixture to minimize voids. While it's impossible to eliminate all voids, the goal is to reduce them as much as possible. Remaining voids can be filled during the hydration of cement and pozzolans [2]. Achieving a continuous particle size distribution helps

reduce the wall effect and the loosening effect. The wall effect refers to disturbances around larger aggregates, common in conventional concrete with crushed stone but not in UHPC. The loosening effect involves the separation of aggregates due to discontinuities in particle size distribution [7].

Another key factor in UHPC formulation is the low water/binder (w/b) ratio, which enhances its compressive strength. Given UHPC's high cement content, mineral additives like silica fume are commonly used. Silica fume is popular due to its high specific surface area and silicon oxide (SiO_2) content, often exceeding 85%, with a specific surface area up to 20,000 m²/kg, earning it the designation of a superpozzolan [8].

Silica is crucial for UHPC's effectiveness; with limited water, cement may not fully hydrate and can act as a filler. Replacing some cement with silica improves efficiency. When in contact with water, silica reacts with calcium hydroxide ($Ca(OH)_2$), a byproduct of cement hydration, to form secondary calcium silicate hydrates (C-S-H), which enhances granular packing and mechanical properties [2].

Another additive discussed in this work, though not commonly used in UHPC, is Marble and Granite Waste (MGW). In Brazil, 10.2 million tons of ornamental rocks were produced in 2021, with granite, marble, and similar stones accounting for 7.0 million tons [9]. Consequently, there is a substantial volume of waste generated from material processing that necessitates proper disposal.

MGW typically accumulates in landfills or designated areas within companies, stemming from the cutting, shaping, and polishing processes of rocks [10]. Generally utilized in civil construction in its wet form (slurry), MGW finds application in concrete blocks, conventional concrete, self-compacting concrete, and mortars [11].

The incorporation of MGW in concrete contributes to inertly filling voids and can accelerate cement hydration, enhancing resistance in the transition zone between aggregate and paste [12]., MGW also improves mixture packing and matrix stability. However, it's crucial to carefully determine replacement proportions based on the mixture components to avoid compromising the overall performance of the composite.

This study aims to investigate UHPC formulations incorporating silica and MGW, alongside various mixing methodologies. The goal is to achieve specific parameters that classify the material as UHPC after 56 days: a fresh state test spread of 270 mm, flexural tensile strength of 6 MPa, and compressive strength of 120 MPa in hardened state tests.

The organization of the article initially presents the materials used and their characteristics. Next, in the methodology section, the characterization of the materials is discussed. Following that, the dosing and mixing methods are addressed. Finally, the methods for analyzing UHPC in both fresh and hardened states are presented. The next section covers the results and discussions. Finally, the article ends with the conclusions and references.

II. MATERIALS

The components selected for the UHPC were chosen based on reference compositions found in the literature. The cement used was CP-V, for its high initial strength, greater durability and resistance to aggressive environments. Natural sand, sieved with particle sizes of 2,36mm in the first phase and 600 µm in the second and third phases, was used.

The silica fume chosen comes from the manufacture of ferrosilicon, with characteristics of a high specific surface area, between 15000m²/kg and 30000m²/kg, and a large amount of silicon dioxide, with a minimum value of 85%. MGW was collected in a tailings pond and subjected to pre-drying in the sun. After drying, the material was manually compiled and subjected to sieving on a 600µm sieve.

Synthetic superplasticizers were initially based on polycarboxylate polymers (SA) and later switched to polycarboxylate ether (SB) after initial testing revealed improved results. SA has density 1.07 g/cm³ and solids content between 30.84% and 31.01%. SB has density between 1.067g/cm³ and 1.107g/cm³ and solids content between 28.5% and 31.5% .

III. METHODOLOGY

3.1 CHARACTERIZATION

The granulometry of the cement and silica was provided by the manufacturer. MGW and sand was characterized. Laser granulometry of MGW was conducted using the Fraunhofer method with 14% obscuration, employing the CILAS 1090 Laser Particle Size Analyzer. To analyze the diameter of the particles, the software "The particle Expert" was used, obtaining the granulometric curve and the parameters d_{10}, d_{50} *e* d_{90}.

Using the X-ray fluorescence method (XRF), it was possible to identify the chemical composition, based on the fluorescence radiation energy emitted by the MGW. The test was carried out in EDX-720 type equipment with a vacuum atmosphere.

X-ray diffraction (XRD) analysis was also carried out. Using this method, it was possible to analyze the presence of crystalline regions or amorphous halos in the material. Cu-ka tube radiation was used, 2Θ scanning range from 5 to 100º. The sweep was 2 degrees/minute, with a current of 30 mA and voltage of 40 kV.

Finally, to understand the morphology of the particles and the production technique of the SAPs, scanning electron microscopy (SEM) was employed using the Hitachi TM 3000. The dried powder samples were subjected to ultrasound for 60 seconds.

For sand, testing procedures and standards adopted are detailed in Table 1.

Table 1. Tests performed and its Regulatory Standards.

Experiment	**Regulatory Standard**
Sieving granulometry	NM 248 (2001) [13]
Determination of organic impurities	NM 49 (2001) [14]
Determination for pulverulent materials content	NM 46 (2001) [15]
Determination of clay lumps and fiable materials content	NBR 7218 (2010) [16]
Determination of density and water absorption	NBR 16916 (2021) [17]
Determination of the unit weight and air-void contents	NBR 16972 (2021) [18]

3.2 DOSAGE AND MIXING

After characterization, the study was divided into three phases based on their chronological execution. Table 2 presents the base formulations for these phases, while Table 3 details the specific changes between each phase, such as variations in additives, the percentage of superplasticizer used, and the water/binder ratio (w/b). Notably, Phase I used substitution for additions, while Phases II and III utilized additional incorporation to reduce w/b and improve compressive strength. Additions were based on mass, with silica added to cement, MGW to sand, and superplasticizer to binders (cement + silica). Method 1, used in Phases I and II, refers to the mixing technique, which was replaced by Method 2 in Phase III. For clarity, for example, the composition M30_S10_SA1.0_0.30 indicates: 30% MGW, 10% silica, SA at 1%, and w/b = 0.30.

Table 2. Mix-designs of references mixtures.

Base dosage – Phase I					
Ciment (kg/m³)	Silica (kg/m³)	Sand (kg/m³)	MGW (kg/m³)	sp (%)	w/b
384.92	VA	448.80	192.34	VA	VA
Base dosage - Phase II					
Ciment (kg/m³)	Silica (kg/m³)	Sand (kg/m³)	MGW (kg/m³)	sp (%)	w/b
571.79	114.36	686.14	343.07	VA	0.25
Final dosage - Phase III					
Ciment (kg/m³)	Silica (kg/m³)	Sand (kg/m³)	MGW (kg/m³)	sp (%)	w/b
571.79	114.36	686.14	343.07	1.50	0.25

Note - VA: Variable according to Table 3

Table 3. Produced dosages of UHPC

Phases	Nomenclature	% sp	Silica	MGW	w/b
Phase I (Mixing Method 1)	M30_S10_SA1.0_0.3	1.00%	10%	30%	0.30
	M30_S15_SA1.0_0.3	1.00%	15%	30%	0.30
	M30_S20_SA1.0_0.3	1.00%	20%	30%	0.30
	M30_S10_SA3.0_0.25	3.00%	10%	30%	0.25
	M30_S10_SA3.5_0.25	3.50%	10%	30%	0.25
	M30_S10_SB3.0_0.25	3.00%	10%	30%	0.25
Phase II (Mixing Method 1)	M50_S20_SB1.0_0.25	1.00%	20%	50%	0.25
	M50_S20_SB1.5_0.25	1.50%	20%	50%	0.25
	M50_S20_SB2.0_0.25	2.00%	20%	50%	0.25
Phase III (Mixing Method 2)	M50_S20_SB1.5_0.25	1.50%	20%	50%	0.25

Mixing Method 1, used in Phases I and II, involved initially mixing binders with half the water and superplasticizer in a tabletop mixer to form a paste. This paste was then transferred to a mortar mixing machine, where inert aggregates, remaining water, and superplasticizer were added. Details are in Table 4. Mixing Method 2, introduced in Phase III, aimed to reduce water loss and improve mixing efficiency. This phase involved changes to the mixer type, mixing times, and speeds, as shown in Table 4.

Table 4. Mixing Methods 1 and 2

Process	Method 1 – Phases I e II			Method 2 – Phase III		
	Action	**Time (sec)**	**Speed (rpm)**	**Action**	**Time (sec)**	**Speed (rpm)**
Paste mixture I and II: Low Rotation Mixer III: Drill with screw attachment for mortar	Initial mixture of 25% water + binders	60	-	Only binders	30	2000
	Cleaning break	30	-	Initial mixture of 50% water + 50% superplasticizer + binders	180	2000
	Mixing of components	60	-			
	Cleaning break and addition of 25% water + 50% superplasticizer	30	-			
	Mixing of all the paste components	120	-	Cleaning break	30	-
Mortar (Mortar mixing machine)	Homogenization of aggregates + absorption water	90	Low	Homogenization of aggregates + absorption water	60	Low
	Paste mixture + aggregates	60	High	Initial paste mixture + aggregates	60	Low
				Paste mixture + aggregates	60	High
	Cleaning break and addition of 50% superplasticizer and the remaining water	30	-	Cleaning break and addition of 50% superplasticizer and 50% water	30	-
	Mixing of components	210	High			
	Cleaning break	30	-			
	Mixing of components	120	High	Mixing of components	390	High

3.3 FRESH STATE AND VOLUMETRIC AND MASS VARIATION

For the fresh state analysis, the Spreadind Test [19] was conducted using a consistency table. The material was poured in three layers with 15, 10, and 5 strokes respectively, into a cone with dimensions

of 130 ± 2 mm at the smaller base, 200 ± 2 mm in height, and 200 ± 2 mm at the larger base. After removing the cone, 30 drops were applied within 30 seconds, and diameters were measured at three different points.

Only for the final dosage, Phase III, the variation in volume and mass of the specimens was analyzed. Using three specimens measuring 22x25x285 mm at ages of 1, 7, and 28 days [20]. Molding was conducted at (23 ± 2) °C and a relative humidity of (60 ± 5)%. Curing conditions were maintained at (23 ± 2) °C with a relative humidity of (50 ± 5)%. Bars were demolded after 48 hours, except for the 1-day test. Dimensional variation (Equation 1) and mass variation (Equation 2) were evaluated.

$$\varepsilon_i = \frac{L_i - L_0}{0{,}25} \qquad (1)$$

$$\Delta m_i = \frac{m_i - m_0}{m_0} \quad (2)$$

Where: ε_i is the dimensional variation, characterized as retraction when less than zero and expansion when positive. L_i is the reading at final age, in mm and L_0 is the reading after demolding. Δm_i is the mass variation m_i is the mass at final age, in grams and m_0 is the mass after deformation, also in grams. For this test, an expansion and retraction comparator was used, with readings taken with the specimen always in the same position.

3.4 HARDENED STATE

For the hardened state analysis, Phases I and II used prismatic forms (40 x 40 x 160 mm) for flexural tensile and compressive strength tests. In Phase III, in addition to prismatic forms, cylindrical specimens (50 x 100 mm) were also used for compression testing. This methodology aimed to reduce deviations observed in the rupture of prismatic specimens. Flexural tensile strength tests were performed using a Shimadzu press with a capacity of up to 10 tons, applying a load rate of 50 N/s with the 3-point method [21]. In Phases I and II, the specimens from this test were then tested for compressive strength using an Amsler press with a capacity of 50 tons at a rate of 500 N/s. Phase III followed a similar procedure, but with cylindrical specimens [21].

In the first two phases, one prismatic specimen was molded for each age group, totaling 3 specimens per dosage, as these phases aimed to define the dosage. In the final phase, three prismatic and three cylindrical specimens were used for each age group. Concrete specimens were demolded after 24 hours and cured in a water and lime solution. Phase I studied ages of 7, 14, and 28 days, focusing on shorter durations for initial testing. Phase II included ages of 7, 28, and 56 days, while Phase III extended to 28, 56, and 91 days to evaluate the material's performance and potential improvements with extended curing times at the final dosage.

IV. RESULTS AND DISCUSSIONS

4.1 CHARACTERIZATION - GRANULOMETRY

The granulometric analysis of the selected materials will be carried out together to assess whether the granulometric distribution of the components is different, promoting a reduction in voids in the mixture. All materials underwent laser granulometry analysis, except for sand, which was subjected to sieving. Cement and silica data were provided by their manufacturers. It can be seen in Figure 1 that cement is the finest material, followed by MGW, silica and sand. It is observed that the particle size distributions are very different, which may favor the packing of the mixture.

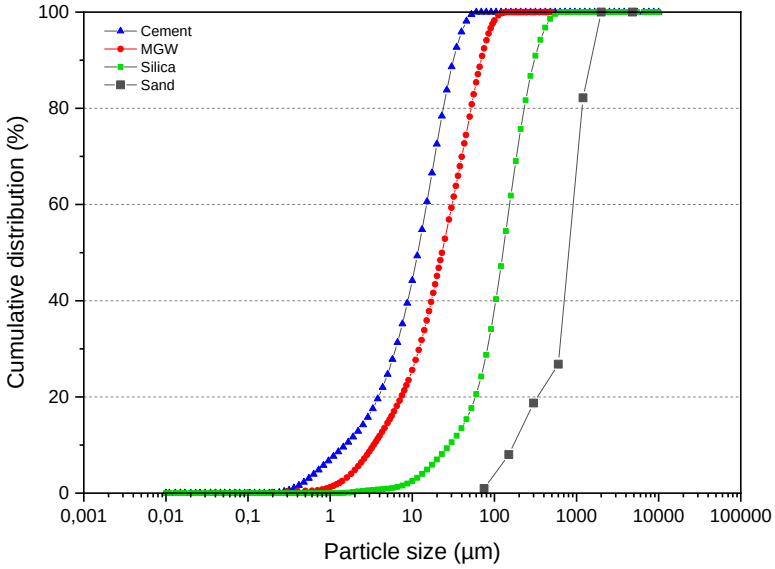

Figure 1. UHPC components diameter

Table 5 details the effective diameter values, specifically D_{10} (diameter at which 10% of the material passes through), D_{50} (median diameter), and D_{90} (diameter at which 90% of the material passes through). The data reveals varying particle sizes among the materials used, which enhances the packaging efficiency of UHPC.

Table 5. Effective diameters of materials used in the study

Material	D_{10}(µm)	D_{50}(µm)	D_{90}(µm)
Cement	1.53	11.68	31.53
MGW	3.39	23.02	69.00
Silica	28.36	126.92	305.87
Sand	90.00	200.00	500.00

4.2 CHARACTERIZATION – SAND

Regarding the organic matter content, Figure 2 shows that the tested solution was only slightly darker than the standard. Using the Hellige reference system, it is concluded that the sand contains insignificant organic matter that would not adversely affect its use in UHPC aggregates.

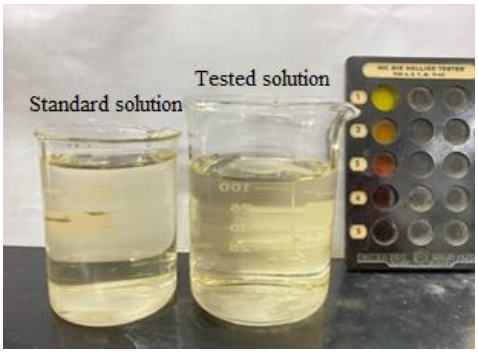

Figure 2. Determination of organic impurities of sand

Table 6 presents other characteristics obtained from sand characterization. The powdery material content was 5%, which includes material with a diameter less than 75 µm, including water-soluble substances, while clay and friable content accounted for 12.8%. Density values fell within the typical range for sand. During batching, the sand exhibited a water absorption of 0.42%, factored into the mixture's water absorption but not considered in the w/b ratio calculation. No characteristics were observed in the sand that could generate setbacks for the concrete.

Table 6. Sand characterization

Pulverulent materials content (%)	5.00
Clay lumps and fiable materials content (%)	12.80
Average density dry condition (g/cm³)	2.47
Average density condition saturated dry surface (g/cm³)	2.48
Average water absorption (%)	0.42

4.3 CHARACTERIZATION – MGW

Based on the fluorescence radiation energy emitted by MGW upon excitation with X-rays, it was possible to identify the chemical elements present in the material. This information is crucial for understanding the waste composition. Table 7 outlines the composition of the MGW under investigation.

Table 7. Chemical composition of MGW by FRX method

Chemical component %	SiO_2	Al_2O_3	Fe_2O_3	K_2O	CaO	MgO	SO_3	SrO	MnO	RB_2O
	66.52	13.05	8.01	7.06	4.06	0.74	0.17	0.15	0.12	0.04

The material predominantly consists of granite residues, considering that granite's composition is 72% SiO2, similar to the chemical composition of the MGW studied [21]. Other observed components are typical in MGW due to the chemical composition of elements found in marble and granite.

Figure 3 presents the mineralogical characterization of MGW using the diffractometry method. Quartz peaks are prominent, especially between 20º and 30º, representing the most abundant material in MGW: SiO2 (ICSD 89278). Peaks of mica (ICSD 84263) and albite (ICSD 68913), common components of granite, were also identified [22]. Additionally, peaks of dolomite (ICSD 10404) and kaolinite (ICSD 84263) were observed, likely originating from marble present in the residue.

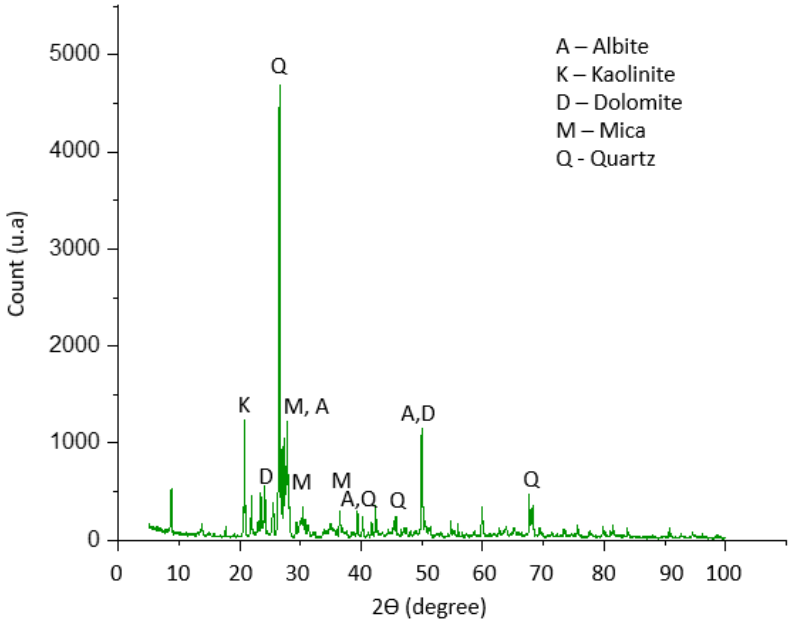

Figure 3. Mineralogical characterization og MGW using the diffractometry method

Figure 4 displays SEM images of MGW. In (a), a 100-fold magnification reveals the irregular and angular morphology of MGW particles, showcasing variability in size and shape due to its nature as a residue, influenced by the original material's cut and composition. At 400x magnification in (b), a particle highlighted by a red arrow exhibits a rough surface texture.

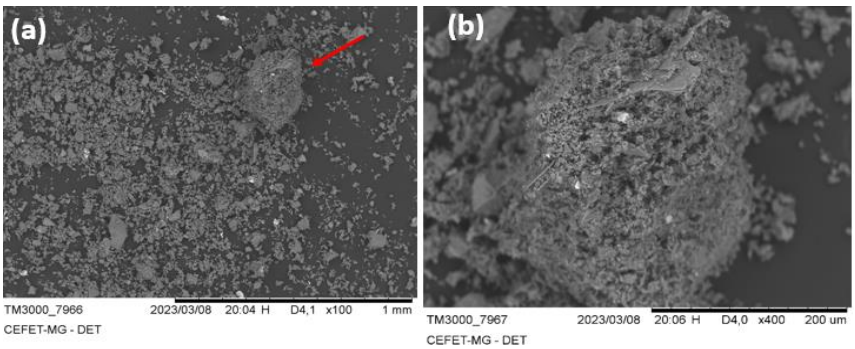

Figure 4. SEM of MGW(a) x110 (b) x400

4.4 ANALYSIS IN THE FRESH STATE AND HARDENED STATE

Initially, MGW was introduced at a 30% replacement rate relative to sand, with silica variations tested at 10%, 15%, and 20%, using 1% superplasticizer and a w/b ratio of 0.30. As shown in Figure 5, all formulations exhibited minimal spread.

Notably, all mixtures with a w/b ratio of 0.30 showed minimal scattering, with the 10% silica dosage achieving the highest value. Since UHPCs typically have a w/b ratio of less than 0.26, a second attempt was made with 10% silica, reducing the w/b ratio to 0.25 and varying the superplasticizer amount. Studies indicate that superplasticizer content in UHPC can reach up to 4%, so 3.0% and 3.5% were tested.

In dosages IV, V, and VI, the increase in superplasticizer was insufficient to achieve the minimum scattering value. This may be due to several factors, such as (i) type and quality of the superplasticizer; (ii) superplasticizer overdose; and (iii) mixing time and application timing of the superplasticizer. Difficulties arise when using superplasticizer with limited water, as inadequate quantity of water

prevents proper dispersion of cement particles [1,7]. Thus, the mixing method, type of superplasticizer, timing of its addition, and w/b ratio all influence the effectiveness of the superplasticizer.

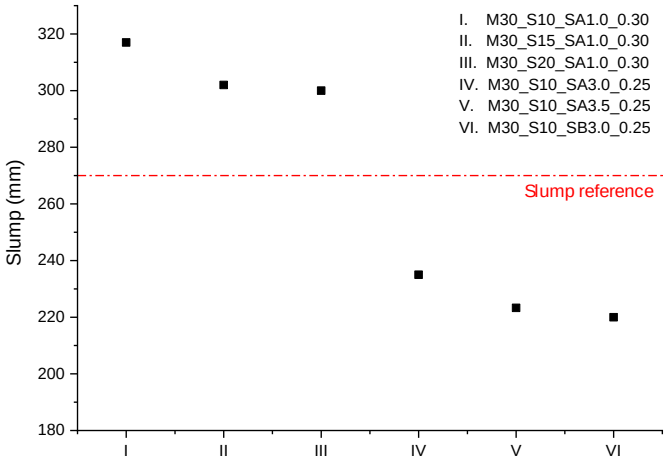

Figure 5. Data obtained for the spreading of dosages - Phase I

Increasing the plasticizer not only reduced the spread but also caused samples with SA to need up to 72 hours for demolding due to insufficient rigidity after 24 hours. This delay may be due to the chemical nature and amount of the superplasticizer used, which slowed the concrete's structural formation. Replacing the SB superplasticizer eased the demolding issue but did not achieve the desired spreading, prompting exploration of alternative methods with SB in later phases.

As shown in Figure 6, flexural tensile strength results I, II, and III exceeded 6 MPa at all ages. There was more consistency between age and resistance in dosages with 15% and 20% silica. For dosages IV, V, and VI, only dosage VI met the predicted minimum. The demolding and curing process for dosages with 3% and 3.5% SA superplasticizer significantly impacted the results.

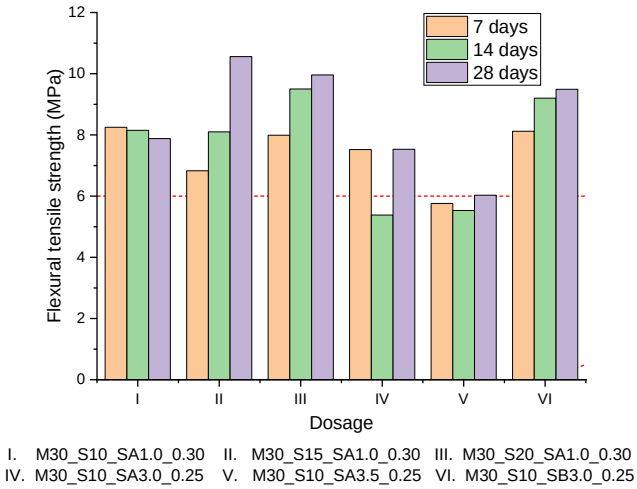

Figure 6. Flexural tensile strength - Phase I

In Figure 7 it is possible to observe the gain in resistance as the percentage of silica increases. The result with 20% silica stands out, which reached higher values after 28 days, but still did not reach the minimum resistance for classification as UHPC. As for the proposal for dosages with a higher superplasticizer content, the same behavior as before is observed, with worse results for dosages with SA. However, there was a drop at 28 days for the use of SB. This behavior is attributed to a failure in the molding process or test execution. Substituting the superplasticizer resulted in a improvement in strength, underscoring the potential of this modification.

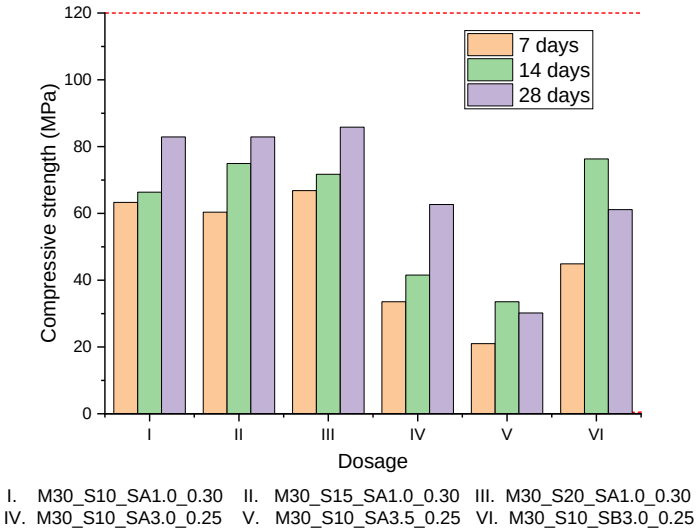

Figure 7. Compressive strength - Phase I

After completing Phase I and analyzing the results, it was decided to use SB superplasticizer at concentrations of 1%, 1.5%, and 2%, and to add 20% silica fume, aiming for a w/b ratio of 0.25. Additionally, changes were made to the sand granulometry (600 µm) and curing time. The 20% silica dosage was chosen due to the good results obtained in the fresh and hardened state and because it provides the greatest amount of binder in the mixture, which could enhance shrinkage resistance.

Figure 8 shows the spread value for Phase II dosing. It is possible to note that 1% superplasticizer proved to be insufficient to obtain the minimum value. The dosages with 1.5% and 2% reached the minimum, with emphasis on the composition with 1.5%. This behavior, as described previously, is related to the search for the ideal dosage of superplasticizer that can act efficiently with the w/b factor of the mixture.

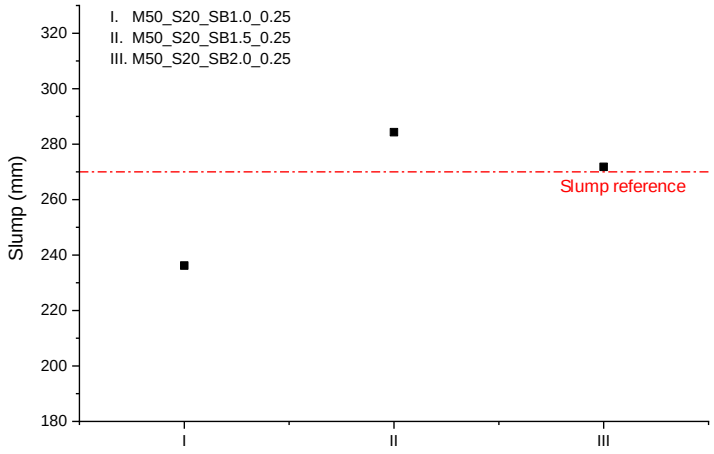

Figure 8. Data obtained for the spreading of dosages – Phase II

All results for flexural tensile strength met the stipulated minimum (Figure 9). Dosages I and II showed less significant gains with age. However, all results were considered favorable considering that the minimum resistance value was obtained after 7 days of curing.

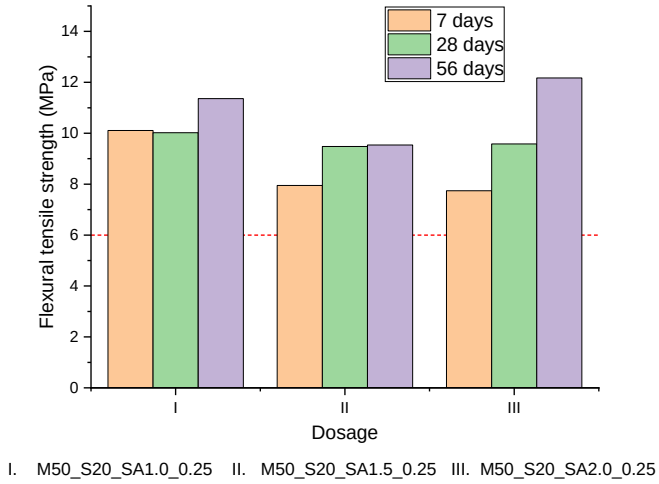

Figure 9. Flexural tensile strength - Phase II

It is noted that the proposed dosage changes brought very significant improvements to compression resistance (Figure 10). All results at 7 days are close to 80 MPa. I and II show results close to 100 MPa at 56 days. Therefore, it is observed that changing the sand size and curing time was beneficial for the study.

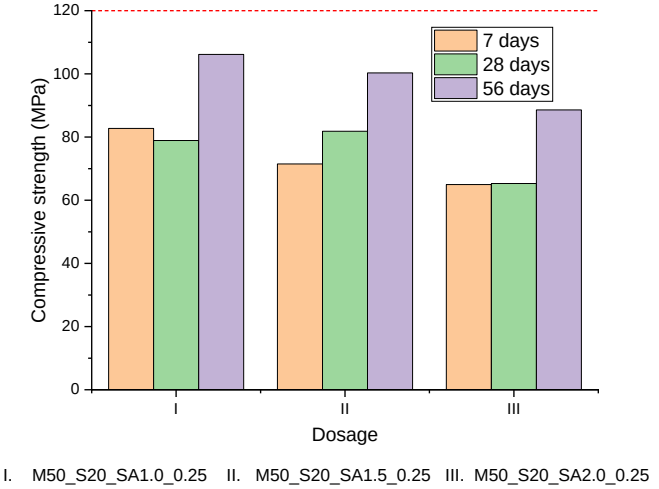

Figure 10. Compressive strength - Phase II

Therefore, knowing that the dosage M50_S20_SB1.5_0.25 presented: (i) a higher scattering value; (ii) the minimum value for flexural strength reached at all ages; and (iii) coherence between resistance and age in the compression analysis, reaching 100 MPa at 56 days, this dosage was chosen for Phase III. To improve the chosen dosage and achieve the parameters for classification as UHPC, adjustments were made to the mortar production process and curing time (28, 56, and 91 days), with the results shown in Figure 11.

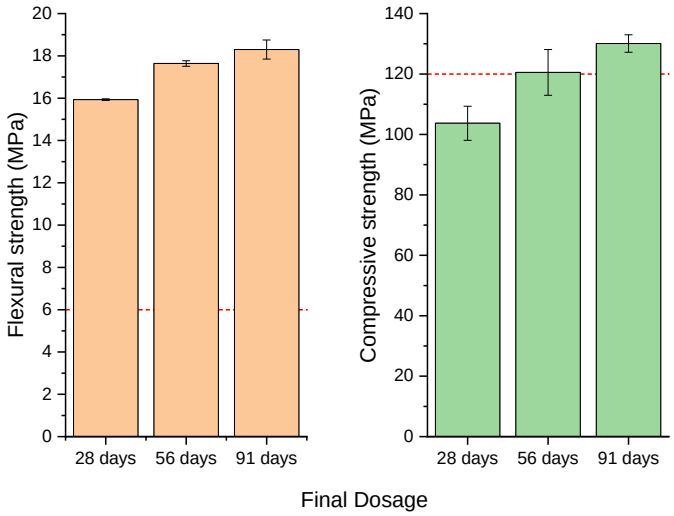

Figure 11. Flexural tensile strength and compressive strength – Final Dosage

The dosage achieved a spread of 284 mm, exceeding the desired 270 mm. In the resistance analysis (Figure 11), the dosage showed flexural tensile strength above the minimum at all ages, reaching 18.3 MPa at 91 days. For compressive strength, it reached 103.7 MPa at 28 days, surpassed the normative minimum at 56 days with 120.5 MPa, and reached 130 MPa at 91 days. Thus, the material met the three criteria for UHPC classification. This highlights the influence of factors like material types, granulometry, superplasticizer type, and mixing method on producing UHPC.

4.5 VOLUMETRIC AND MASS VARIATION

Finally, the volumetric and mass variation of the UHPC obtained was analyzed, as shown in Figure 12. It was observed that the specimen shrank with the evolution of the curing process. This behavior may be linked to drying shrinkage and autogenous shrinkage, which are very common in UHPCs due to the low w/b factor. The mass variation obtained was consistent with the volume variations. These variations are understood to be linked to the loss of water from the material during the curing process.

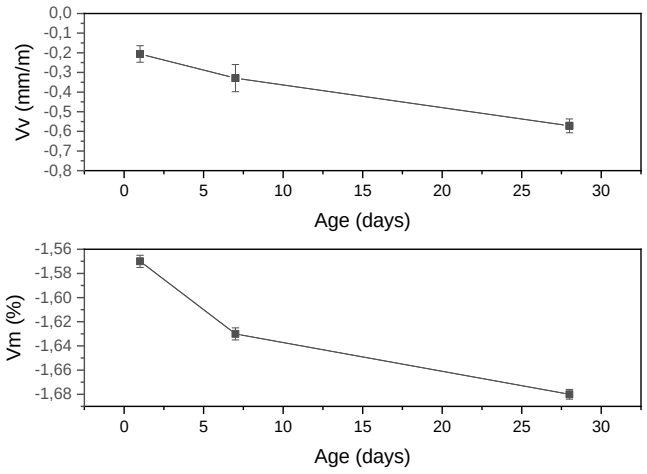

Figure 12. Volumetric and mass variation – Final Dosage

V. CONCLUSIONS

In summary, this study provided a detailed analysis of UHPC dosing, investigating both the behavior in the fresh state and the mechanical properties in the hardened state with the addition of silica and MGW. The influence of curing times, types and percentages of superplasticizer, as well as production

methods, were evaluated. This allowed for an observation of how the constituent materials and their proportions impact the desired characteristics of UHPC. The additions of silica and MGW improved the matrix packaging, increasing the workability and resistance of the UHPC, especially at more advanced ages. This demonstrates the potential for future work, such as the addition of fibers.

ACKNOWLEDGEMENTS

To the AECem research network (Advanced Eco-Efficient Cement-Based Technologies) for their valuable contributions to the research, to the Research Support Foundation of the State of Alagoas for financial support (FAPEAL), and to the Federal University of Alagoas and the Federal Institute of Alagoas for infrastructure and team support.

REFERENCES

[1]. Fan D., Zhu J., Fan M., Lu J., Chu S. H., and Dong E., (2003) "Intelligent design and manufacturing of ultra-high performance concrete (UHPC) – A review," vol. 385.

[2]. Christ R., B. & Tutiakian, P. Helene, (2022) "Concreto de ultra alto desempenho: UHPC - Fundamentos, propriedades e dosagem," 1ª ed. São Paulo.

[3]. Zhu Y., Zhang Y., Hussein H. H., & Chen G., (2020) "Flexural strengthening of reinforced concrete beams or slabs using ultra-high performance concrete (UHPC): A state of the art review," Eng Struct, vol. 205, p. 110035, doi: 10.1016/j.engstruct.2019.110035.

[4]. Perry V. H. & America N., (2020) "What Really is Ultra-High Performance Concrete? Towards a Global Definition," [Online]. Available: https://www.researchgate.net/publication/340441896.

[5]. Li J., Wu Z., Shi C., Yuan Q., & Zhang Z., (2020) "Durability of ultra-high performance concrete – A review," Construction and Building Materials, vol. 255. Elsevier Ltd. doi: 10.1016/j.conbuildmat.2020.119296.

[6]. Manzano M. A. Silva R., E. F. da, Lopes A. N. de M., & Tolêdo Filho R. D., (2021) "Mecanismo de atuação dos Polímeros Superabsorventes como agentes de cura interna para mitigar a retração autógena em Concretos de Alta Resistência (CAR) – Estado da Arte," Matéria (Rio de Janeiro), vol. 26, no. 2, doi: 10.1590/s1517-707620210002.1256.

[7]. De Larrard F. & Sedran T., (2002) "Mixture proportioning of high-performance concrete," Cem Concr Res, vol. 32, no. 11, pp. 1699–1704, doi: 10.1016/S0008-8846(02)00861-X.

[8]. Silva V., M. G.; Battagin & Gomes A. F. (2017), "Cimento Portland com Adições Minerais," in Concreto: Ciência e Tecnologia, São Paulo, p. p.793-841.

[9]. Associação Brasileira da Indústria de Rochas Ornamentais – ABIROCHAS (2021), "Balanço das exportações e importações brasileiras de materiais rochosos naturais e artificiais de ornamentação e revestimento em 2021." Brasília, p. 17. [Online]. Available: chrome-extension://efaidnbmnnnibpcajpcglclefindmkaj/https://abirochas.com.br/wp-content/uploads/2022/03/Informe-01_2022-Exportacoes-2021.pdf

[10]. Singh M., Choudhary K., Srivastava A., Singh Sangwan K., & Bhunia D. (2017), "A study on environmental and economic impacts of using waste marble powder in concrete," Journal of Building Engineering, vol. 13, no. July, pp. 87–95, doi: 10.1016/j.jobe.2017.07.009.

[11]. Pereira M. M. L., Capuzzo V. M. S., & Lameiras R. de M. (2022), "Evaluation of use of marble and granite cutting waste to the production of self-compacting concrete," Constr Build Mater, vol. 345, no. February, p. 128261, doi: 10.1016/j.conbuildmat.2022.128261.

[12]. Galetakis M. & Soultana A. (2016), "A review on the utilisation of quarry and ornamental stone industry fine by-products in the construction sector," Constr Build Mater, vol. 102, pp. 769–781, doi: 10.1016/j.conbuildmat.2015.10.204.

[13]. ASSOCIAÇÃO BRASILEIRA DE NORMAS TÉCNICAS. (2001), NBR NM 248 – Agregados - Determinação da composição granulométrica. Rio de Janeiro.

[14]. ASSOCIAÇÃO BRASILEIRA DE NORMAS TÉCNICAS. (2001), NM 49 . Agregado miúdo. Determinação de impurezas orgânicas. Rio de Janeiro 2001.

[15]. ASSOCIAÇÃO BRASILEIRA DE NORMAS TÉCNICAS. (2001), NM 46 . Agregados - Determinação do material fino que passa através da peneira 75 µm, por lavagem. Rio de Janeiro.

[16]. ASSOCIAÇÃO BRASILEIRA DE NORMAS TÉCNICAS. (2010), NBR 7218 . Agregados — Determinação do teor de argila em torrões e materiais friáveis. Rio de Janeiro.

[17]. ASSOCIAÇÃO BRASILEIRA DE NORMAS TÉCNICAS. (2021), NBR 16916 . Agregado miúdo - Determinação da densidade e da absorção de água. Rio de Janeiro.

[18]. ASSOCIAÇÃO BRASILEIRA DE NORMAS TÉCNICAS. (2021), NBR 16972 . Agregado miúdo - Determinação da densidade e da absorção de água. Rio de Janeiro.

[19]. ASSOCIAÇÃO BRASILEIRA DE NORMAS TÉCNICAS. (2016). NBR 13276. Argamassa para assentamento e revestimento de paredes e tetos - Determinação do índice de consistência. Rio de Janeiro.

[20]. ASSOCIAÇÃO BRASILEIRA DE NORMAS TÉCNICAS. (2005), NBR 15261. Argamassa para assentamento e revestimento de paredes e tetos - Determinação da variação dimensional (retratação ou expansão linear). Rio de Janeiro.

[21]. ASSOCIAÇÃO BRASILEIRA DE NORMAS TÉCNICAS. (2005). NBR 13279. Argamassa para assentamento e revestimento de paredes e tetos - Determinação da resistência à tração na flexão e à compressão. Rio de Janeiro.

[22]. Barbosa K. S. L., Carneiro M. de S., Souza J. A. da S., Costa D. da S., & Mâcedo E. N., (2022) "Resíduos de mármore e granito em materiais compósitos: relação da granulometria nas propriedades mecânicas," Conjecturas, vol. 22, no. 2, pp. 1319–1331 , doi: 10.53660/conj-833-f04.

Authors

Priscila de Souza Maciel graduated in Civil Engineering from the Federal University of Ouro Preto (2015) and a master's degree in Geotechnics (Research Line: Rigid Pavement Infrastructure with Steel Fiber Reinforcement) from the same institution (NUGEO/UFOP), completed in 2017. Worked at IFPB in 2020 and is currently a full professor at the Federal Institute of Alagoas, Campus Coruripe, teaching in the technical building course and pursuing a Ph.D. in Materials Science at the Federal University of Alagoas. Interested in the following topics: paving, UHPC, fiber-reinforced concrete, SAP

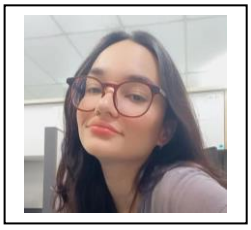

Maria Luiza Malta da Rocha Silva undergraduate student in Civil Engineering at the Federal University of Alagoas - A. C. Simões Campus. Researcher in the field of Materials.

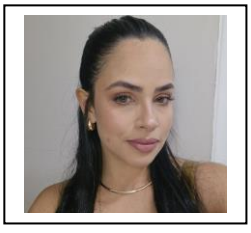

Ingrid Vieira Fernandes Monteiro pharmacist from the Federal University of Alagoas. Master's degree in Pharmaceutical Sciences from the Postgraduate Program in Pharmaceutical Sciences at UFAL (PPGCF-UFAL). Currently, PhD student in Material Sciences (UFAL). She has experience in nanotechnology, with an emphasis on the development and characterization of polymeric nanocomposites and nanostructured bioinsecticide formulations.

Paulo Cesar Correia Gomes. Graduated in Civil Engineering from the Federal University of Alagoas. Master's in Civil Engineering from the Federal University of Rio de Janeiro. PhD from the Polytechnic University of Catalonia - Building Engineering. Post-doctorate from the Polytechnic School of the University of São Paulo. Professor at the Federal University of Alagoas. Research in Civil Engineering, with an emphasis on concrete technology, special concretes and non-conventional materials, working mainly on the subjects: construction waste, self-compacting concrete, lightweight concrete, fiber concrete, eco-efficient concrete, sustainable technology and construction elements.